

Observing Supernova 1987A with the Refurbished Hubble Space Telescope

Kevin France^a, Richard McCray^b, Kevin Heng^{c,d}, Robert P. Kirshner^e, Peter Challis^e, Patrice Bouchet^f, Arlin Crotts^g, Eli Dwek^h, Claes Franssonⁱ, Peter M. Garnavich^j, Josefin Larsson^k, Peter Lundqvist^l, Nino Panagia^{k,l,m}, Chun S. J. Punⁿ, Nathan Smith^o, Jesper Sollermanⁱ, George Sonneborn^h, John T. Stocke^a, J. Craig Wheeler^p

^aCenter for Astrophysics and Space Astronomy, University of Colorado, Boulder, CO 80309-0389, U.S.A.

^bJILA, University of Colorado, Boulder, CO 80309-0440, U.S.A.

^cInstitute for Advanced Study, School of Natural Sciences, Einstein Drive, Princeton, NJ 08540, U.S.A.

^dETH Zürich, Institute for Astronomy, Wolfgang-Pauli-Strasse 27, CH-8093, Zürich, Switzerland

^eHarvard-Smithsonian Center for Astrophysics, 60 Garden Street, Cambridge, MA 02138, U.S.A.

^fService d'Astrophysique DSM/IRFU/Sap CEA - Saclay, Orme des Merisiers, FR 91191 Gif-sur-Yvette, France

^gDepartment of Astronomy, Mail Code 5240, Columbia University, 550 W. 120th St., New York, NY 10027, U.S.A.

^hNASA Goddard Space Flight Center, Code 665, Greenbelt, MD 20771, U.S.A.

ⁱDepartment of Astronomy, The Oskar Klein Centre, Stockholm University, 106 91 Stockholm, Sweden

^j225 Nieuwland Science, University of Notre Dame, Notre Dame, IN 46556-5670, U.S.A.

^kSpace Telescope Science Institute, 3700 San Martin Drive, Baltimore, MD 21218, U.S.A.

^lINAF/CT, Osservatorio Astrofisico di Catania, Via S. Sofia 78, I-95123 Catania, Italy

^mSupernova Ltd, OYV #131, Northsound Road, Virgin Gorda, British Virgin Islands

ⁿDepartment of Physics and Center for Theoretical and Computational Physics, The University of Hong Kong, Pok Fu Lam Road, Hong Kong, China

^oDepartment of Astronomy, University of California, Berkeley, CA 94720-3411, U.S.A.

^pDepartment of Astronomy, University of Texas, Austin, TX 78712-0259, U.S.A.

Abstract

The young remnant of supernova 1987A (SN 1987A) offers an unprecedented glimpse into the hydrodynamics and kinetics of fast astrophysical shocks. We have been monitoring SN 1987A with the *Hubble Space Telescope* (HST) since it was launched. The recent repair of the *Space Telescope Imaging Spectrograph* (STIS) allows us to compare observations in 2004, just before its demise, with those in 2010, shortly after its resuscitation by NASA astronauts. We find that the Ly α and H α lines from shock emission continue to brighten, while their maximum velocities continue to decrease. We report evidence for nearly coherent, resonant scattering of Ly α photons (to blueshifts $\sim -12,000$ km s⁻¹) from hotspots on the equatorial ring. We also report emission to the red of Ly α that we attribute to N v $\lambda\lambda 1239, 1243$ Å line emission. These lines are detectable because, unlike hydrogen atoms, N⁴⁺ ions emit hundreds of photons before they are ionized. The profiles of the N v lines differ markedly from that of H α . We attribute this to scattering of N⁴⁺ ions by magnetic fields in the ionized plasma. Thus, N v emission provides a unique probe of the isotropization zone of the collisionless shock. Observations with the recently installed *Cosmic Origins Spectrograph* (COS) will enable us to observe the N v $\lambda\lambda 1239, 1243$ Å line profiles with much higher signal-to-noise ratios than possible with STIS and may reveal lines of other highly ionized species (such as C iv $\lambda\lambda 1548, 1551$ Å) that will test our explanation for the N v emission.

Key words: hydrodynamics – shock waves – supernovae: individual (SN 1987A) – ISM: supernova remnants – ultraviolet: general

1. Introduction

The death of a massive star produces a violent explosion known as a supernova (SN), which expels matter at hypersonic velocities. The shock impact of the supernova debris with ambient matter creates a radiating system known as a supernova remnant. SN 1987A (23 February 1987), the brightest such event observed since Kepler's supernova (SN 1604) [1], gives us a unique opportunity to witness the development of a supernova remnant [2, 3]. Because of its proximity (in the Large Magellanic Cloud), we can resolve the interaction of its shocks with circumstellar matter using the recently repaired (ACS) and installed (WFC3) imaging cameras, and the recently revived imaging spectrograph (STIS) on the *Hubble Space Telescope* (HST). The most remarkable feature of the circumstellar matter is a relatively dense ($n_{\text{H}} \sim 10^3\text{--}10^4$ atoms cm⁻³) equatorial ring of diameter 1.34 light years (lt-yr), inclined at an angle $i = 45^\circ$ with respect to the line of sight [4, 5, 6]. This ring is believed to be produced by a mass loss event that occurred about 20,000 years before the supernova explosion [7, 8].

Email addresses: Kevin.France@colorado.edu (Kevin France), dick@jila.colorado.edu (Richard McCray), heng@ias.edu (Kevin Heng), rkirshner@cfa.harvard.edu (Robert P. Kirshner), pchallis@cfa.harvard.edu (Peter Challis), patrice.bouchet@cea.fr (Patrice Bouchet), arlin@astro.columbia.edu (Arlin Crotts), eli.dwek@nasa.gov (Eli Dwek), claes@astro.su.se (Claes Fransson), pgarnavi@nd.edu (Peter M. Garnavich), josefin.larsson@astro.su.se (Josefin Larsson), peter@astro.su.se (Peter Lundqvist), panagia@stsci.edu (Nino Panagia), jcsun@hkucc.hku.hk (Chun S. J. Pun), nathans@astro.berkeley.edu (Nathan Smith), jesper@astro.su.se (Jesper Sollerman), george.sonneborn-1@nasa.gov (George Sonneborn), stocke@casa.colorado.edu (John T. Stocke), wheel@astro.as.utexas.edu (J. Craig Wheeler)

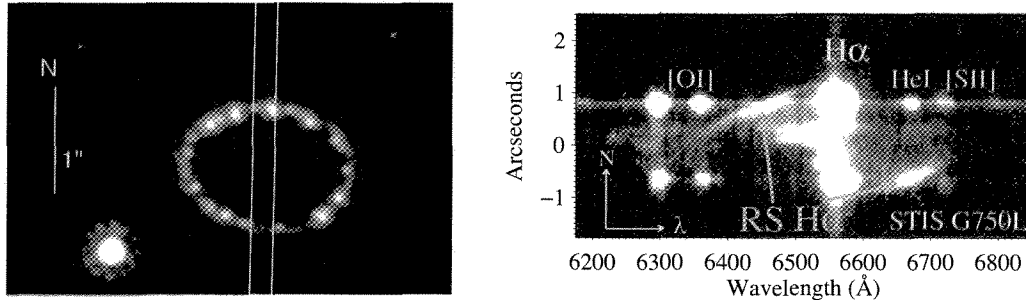


Figure 1: (left) *HST*-ACS F625W image illustrating the slit orientation used in this study (G140L and G750L). Use of the $52'' \times 0.2''$ slit reduces spatial-velocity confusion in the observed two-dimensional spectra. This optical image is dominated by $H\alpha$, and is displayed with north up and east to the left. (right) *STIS* G750L spectrum of SN 1987A obtained on 31 January 2010. The vertical bar at the center of the image is stationary $H\alpha$ emission from interstellar or circumstellar gas, aligned to be at roughly the same height as the optical image shown on the left. The bright spots at the north and south of this bar are due to $H\alpha + [N II] \lambda\lambda 6548, 6583$ Å emission from hotspots on the equatorial ring. The pairs of dots to the left are due to $[O II] \lambda\lambda 6300, 6364$ Å emission from the equatorial ring and the fainter ones on the right are due to $He I \lambda 6678$ Å and $[S II] \lambda\lambda 6716, 6731$ Å. The blueshifted streaks near the center are $H\alpha$ emission excited by radioactivity in the interior of the supernova debris. (The redshifted counterpart of this emission is obscured by internal dust in the debris.) The curved, blueshifted streak extending from the north side of the vertical bar and the redshifted streak on the south side (noted with orange arrows) are $H\alpha$ emission from the brightest parts of the reverse shock (RS). This shock emission peaks between $|v_z| \approx 4000\text{--}6000$ km s $^{-1}$. These portions of the streaks are produced by hydrogen atoms crossing the reverse shock just inside the equatorial ring on the north and south sides, respectively. The Doppler shifts are in the range expected from freely expanding debris crossing a shock surface located at radius of $r \approx 0.6$ lt-yr.

The rapidly expanding debris of the supernova explosion interacts hydrodynamically with circumstellar matter. If the circumstellar matter has a smooth (uniform or power-law) density distribution, a double-shock structure will be established [9]. A forward shock (blast wave) propagates into the circumstellar matter, creating a layer of hot, shocked gas. The pressure of this layer drives a reverse shock into the supernova debris. This double-shock structure propagates outwards until the blast wave encounters a relatively dense obstacle (such as the circumstellar ring), in which case it will suddenly slow down, creating a reflected shock that will propagate backwards and merge with the reverse shock.

The first evidence of interaction of the blast wave with the equatorial ring appeared in 1995, when a rapidly brightening optical “hotspot” appeared in images taken with the *WFPC2* camera aboard the *HST* [10, 11]. A few years later, three more hotspots appeared. Today, the ring is encircled by about 30 hotspots (Figure 1). Located just inside the ring, the long duration of these localized emission regions suggest that they are dense fingers protruding inwards from the equatorial ring. The origin of these fingers has yet to be adequately explained. The hotspots manifest the optical emission by the dense gas that is shocked by the blast wave as it enters the fingers [12].

In this paper, we present new and archival observations from *HST*-*STIS*. The new observations (Section 2) were made following the repair of the *STIS* instrument during the *Hubble* servicing mission in May 2009. In Section 3, we describe the shape and evolution of the reverse shock, as traced by $H\alpha$ emission. In Section 4, we present evidence for nearly coherent scattering of Ly α photons from hotspots in the ring, and in Section 5 we report the detection of a faint emission feature from the reverse shock that we attribute to redshifted N v $\lambda\lambda 1239, 1243$ Å emission. In Section 6, we describe how observations with the new *Cosmic Origins Spectrograph* (COS) aboard the *HST* will enable us to observe these phenomena in greater detail and to test our interpretation through observations of other ultraviolet lines such as C iv $\lambda\lambda 1548, 1551$ Å.

2. New Observations from the Space Telescope Imaging Spectrograph

The *Supernova 1987A Intensive Study* (SAINTS) is a sustained *Hubble* project (P.I.: R.P. Kirshner) to track and interpret the temporal, spatial, and spectral evolution of SN 1987A. The SAINTS program includes long-term ultraviolet/optical monitoring with *STIS* (over the $\sim 1150\text{--}9000$ Å bandpass), which was repaired in May 2009 by the astronaut crew of the STS-125/Servicing Mission 4.

In the present analysis, we include results from the last epoch of our *STIS* observations (18–23 July 2004) prior to instrument’s failure in August 2004 and our first results from the recently repaired instrument, made on 31 January 2010. The 2004 observations were presented by Heng et al. [13]. The *STIS* G140L ($\Delta\lambda = 1.2$ Å) and G750L ($\Delta\lambda = 9.8$ Å) modes, with the $52'' \times 0.2''$ slit, were used to observe SN 1987A on 31 January 2010 for total exposure times of 8612 s and 14200 s, over six and ten exposures, respectively. These exposures were taken parallel to the north-south ring axis (Figure 1; see also Figure 1 of [13]), centered on R.A. = $05^h 25^m 28.11^s$, Dec. = $-69^\circ 16' 11.1''$ (J2000) in the Large Magellanic Cloud. The optical image shown at left in Figure 1 was obtained with the *Advanced Camera for Surveys* (ACS) on 28 November 2003, in the F625W filter, with an exposure time of 800 s.

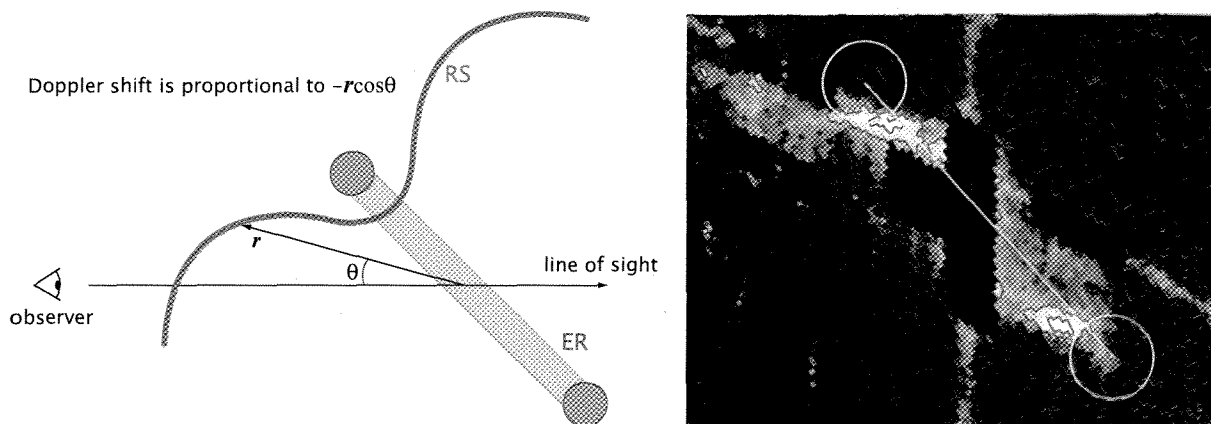


Figure 2: (left) Schematic illustration of the location of the reverse shock (RS) with respect to the equatorial ring (ER), which is inclined 45° to the line of sight. The velocity of the freely expanding supernova debris inside the reverse shock projected along the observer's line of sight is proportional to $-r \cos \theta$. (right) $H\alpha$ emission, from the reverse shock, transformed into a cross-sectional view through the circumstellar ring (see text). The diameter of the equatorial ring (the distance between the centers of the yellow circles) is 1.34 lt-yr. The left and right yellow circles represent the near (N) and far (S) sides of the equatorial plane of the ring, respectively. To keep the focus on the reverse shock, emission features from the ring and hotspots have been blacked out. The circles represent the cross section of the ring, and contours highlight the emission peaks on the northern and southern streaks. The reverse shock emission peaks just inside of the equatorial ring, on the near side of the equatorial plane.

3. $H\alpha$ Emission

Radiation from the reverse shock can be observed at optical and ultraviolet wavelengths. Before it reaches the reverse shock, the outer layer of the supernova debris consists mostly of partially ionized hydrogen and helium gas that has been expanding freely since the explosion. When neutral hydrogen atoms cross the reverse shock, they are excited and ionized by collisions with electrons, protons, and helium nuclei in the hot, shocked plasma. If the atoms are excited before they are ionized, they will produce emission in the $Ly\alpha$ (1216 Å) and $H\alpha$ (6563 Å) lines. On average, approximately 1 $Ly\alpha$ photon and 0.2 $H\alpha$ photons are produced for every hydrogen atom crossing the reverse shock [14, 15, 16].

The emission properties of the reverse shock in SN 1987A are similar to the Balmer-dominated shock emission observed in several Galactic and Large Magellanic Cloud supernova remnants, where photons are produced via collisional excitation (and charge exchange) rather than recombination [14, 17, 18]. The difference is that in the case of other supernova remnants, the supernova blast wave overtakes nearly stationary hydrogen gas in circumstellar matter, while in the case of SN 1987A, fast-moving hydrogen gas in the supernova debris overtakes the reverse shock. As the hydrogen atoms in the supernova debris cross the reverse shock, they freely stream with radial velocity $v_r = r/t_e$, where r is the radius of the reverse shock measured from the explosion center and t_e is the time since the explosion. Likewise, the atoms have Doppler velocity (projected along the line of sight) $v_z = -r \cos \theta / t_e$, where θ is the angle between the streaming supernova debris and the line of sight to the observer. When they are excited by collisions with the shocked gas, the hydrogen atoms are not deflected, so the Doppler shifts of the resulting emission lines we observe correspond to the projected ballistic velocity of the unshocked supernova debris. For instance, at $t_e = 23$ yr, the Doppler velocity of supernova debris crossing the reverse shock normal to the equatorial plane and located at $r = 0.6$ lt-yr, slightly inside the equatorial ring, is $v_z = -0.6 c \cos 45^\circ / 23 = 5530 \text{ km s}^{-1}$ (Figure 2).

Figure 1 shows a portion of the *STIS* G750L spectrum, centered about the $H\alpha$ emission line, from the 31 January 2010 observations. The panel on the left shows the location of the slit superposed on an image of the supernova dominated by $H\alpha$ emission. The equatorial ring is tilted such that north is nearest to the observer and south is farthest. Therefore, the $H\alpha$ and $Ly\alpha$ emission lines from the reverse shock are blueshifted on the north side and redshifted on the south side.

As there is a unique mapping between distance along the line of sight and Doppler shift, one can convert the spectrum of Figure 1 to a tracing of the location of the reverse shock in depth. This conversion is illustrated in Figure 2. Note that the $H\alpha$ emission from the reverse shock is highly concentrated just inside the equatorial ring, because the reverse shock penetrates into the deeper (hence denser) supernova envelope at the equatorial plane, where it is held back by shocks reflected from the ring.

The net $H\alpha$ flux observed through the $52'' \times 0.2''$ slit in the total reverse shock (northern blueshifted plus southern redshifted streaks) in Figure 1 (right) is $3.3 (\pm 0.5) \times 10^{-13} \text{ ergs cm}^{-2} \text{ s}^{-1}$. This value is a factor of about 1.7 greater than the corresponding value measured in July 2004 [13]. Aperture size and alignment differences preclude a direct comparison, but the increase in $H\alpha$ emission observed with *STIS* is essentially equal to the ratio (1.67) of our 2010 observations to those from February 2005 ground-based observations with the *Magellan Telescope* [19]. This increase is consistent with an extrapolation using the predicted trend.

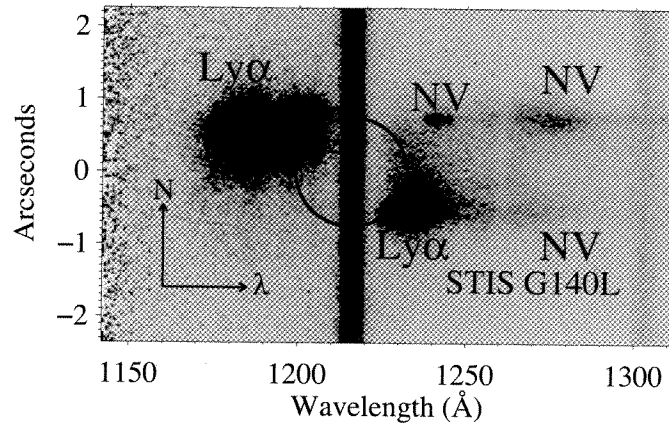


Figure 3: *STIS* G140L observations of SN 1987A, acquired on 31 January 2010. North is up. Prominent reverse shock emission features in the 1142–1312 Å bandpass are labeled. The bright vertical stripe is the slit image in geocoronal Ly α . The yellow ellipse approximates the location of the circumstellar emission ring. Broad, faint features seen on the north and south sides between ~ 1260 – 1290 Å (labeled N v in yellow) are produced by nitrogen ions in the reverse shock. The narrow feature labeled N v in magenta is due to shock-excited N v emission from hotspots on the N side of the ring that fall within the *STIS* $52'' \times 0.2''$ slit.

4. Ly α Emission

Figure 3 shows the spectrum of SN 1987A taken through the same $0.2''$ slit as in Figure 1 in the vicinity of Ly α with the G140L mode of *STIS*. This spectrum is more complicated than that of Figure 1 because, unlike H α photons, Ly α photons experience nearly coherent resonant scattering by hydrogen atoms. For example, Ly α emission is absent at wavelengths immediately blue- and redward of the slit because of absorption by hydrogen atoms in the Milky Way and Large Magellanic Cloud. Furthermore, the broad Ly α emission is not confined to a narrow strip delineating the reverse shock surface, unlike in the case of H α .

Figure 4 shows comparisons of one-dimensional scans of the Ly α (the dark streaks in Figure 3) and H α (the bright streaks in Figure 1) emission from the reverse shock. The observed H α and Ly α fluxes have been increased by factors ≈ 1.5 and 8, respectively, to correct for interstellar extinction along the line of sight to SN 1987A [20, 21]. In the northern Ly α velocity distribution (Figure 4, *left*), we see that the ratio of Ly α :H α photon fluxes has a fairly constant value near 40 for velocities between -2500 km s $^{-1}$ and -6000 km s $^{-1}$. This ratio is much greater than the expected photon production ratio of 5:1 for a Balmer-dominated shock [15, 16], partly because we are considering spatial regions where Ly α emission is diffuse (but bright) and H α emission is faint. Moreover, the H α emission fades for blueshift velocities $< -8,000$ km s $^{-1}$, while the Ly α emission remains bright to blueshift velocities approaching $-12,000$ km s $^{-1}$. (Gröningsson et al. [6] observed broad H α emission extending from $-13,000$ km s $^{-1}$ to $+13,000$ km s $^{-1}$ in a spectrum taken in October 2002 with the *European Southern Observatory Very Large Telescope*, but the high velocity wings they observed are below the noise level in the *STIS* spectrum.) If the Ly α photons are produced by the same mechanism as the H α photons, then the Ly α :H α ratio should be the same for all observed velocities; but it is not. Therefore, we conclude that most of the observed Ly α emission cannot be produced directly by hydrogen atoms crossing the reverse shock.

Instead, we propose a different mechanism to account for most of the highly blueshifted Ly α emission. As the supernova blast wave enters the equatorial ring, the shocked hotspots on the ring become bright sources of Ly α radiation. This radiation is invisible to observers on Earth because it is centered at zero velocity with respect to the interstellar neutral hydrogen and its linewidth is narrow ($\Delta v < 300$ km s $^{-1}$) [6, 12], so that it is entirely blocked by interstellar absorption. Roughly half of this radiation propagates inwards into the supernova debris, where the Ly α photons may be resonantly scattered by hydrogen atoms that are expanding with radial velocities ranging from 3000 km s $^{-1}$ to 9000 km s $^{-1}$. Consider the blueshifted emission from the north side. In the rest frame of the hydrogen atoms in the expanding debris, photons propagating inwards are blueshifted. If they are then scattered backwards towards Earth, they will be blueshifted a second time.

Figures 3 and 4 show that there is no corresponding bright, high-velocity, redshifted Ly α component on the south side of the image. The Ly α photons which are emitted radially inwards by the ring hotspots on the south side are seen as blueshifted by hydrogen atoms in the onrushing debris. However, unlike the case in the north, the photons scattered towards the observer receive a redshift that tends to cancel out this blueshift, resulting in a near-zero net velocity shift. On the other hand, Ly α photons emitted by the ring in a direction sideways compared to the debris will be redshifted by a velocity corresponding to the projected velocity of the debris if they are scattered toward the observer.

To check the plausibility of such a mechanism, we should verify that a sufficient number of Ly α photons are emitted by the hotspots to account for the observed high-velocity Ly α and that the neutral hydrogen layer in the expanding supernova envelope has sufficient optical depth to scatter Ly α photons by roughly half of the observed maximum velocity, *i.e.*, 6000 km s $^{-1}$. One cannot measure the emitted Ly α flux from the hotspots directly because, as mentioned above, this radiation is blocked by interstellar

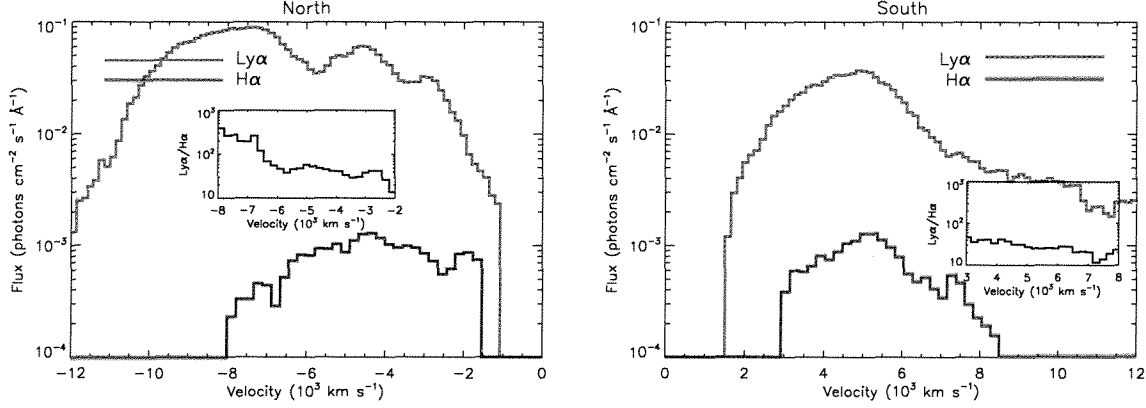


Figure 4: (*left*) Integrated $H\alpha$ and $Ly\alpha$ emission from the reverse shock on the north side of the equatorial ring. While the $H\alpha$ emission approaches zero blueward of -8000 km s^{-1} , it has been artificially truncated in this plot because of strong contamination from $[O \text{ I}] \lambda\lambda 6300, 6364 \text{ \AA}$ present in the hotspot (see Figure 1). The inset shows the ratio of $Ly\alpha:H\alpha$. The broad dip in the $Ly\alpha$ emission near -6000 km s^{-1} may be due to absorption by interstellar $Si \text{ II}$ ($\lambda\lambda 1190, 1193 \text{ \AA}$). Interstellar absorptions from $Si \text{ II}$ ($\lambda\lambda 1190, 1193 \text{ \AA}$, $\lambda\lambda 1260, 1265 \text{ \AA}$ and $\lambda\lambda 1526, 1533 \text{ \AA}$) are clearly detected on the sightline to a nearby star; however, a quantitative comparison is precluded by the low resolution of the *STIS* G140L mode and the comparison between filled slit and point source observations. (*right*) We see a similar pattern in the southern, redshifted emission. We truncate the southern $H\alpha$ profile at $v \geq 8500 \text{ km s}^{-1}$ because the $H\alpha$ flux at these velocities is consistent with a combination of detector background and $[S \text{ II}]$ emission scattered inside of the equatorial ring radius.

hydrogen atoms. However, we can instead measure the direct $H\alpha$ emission from the ring and apply a theoretical scaling ($Ly\alpha:H\alpha \sim 5 - 10$; [22]) to obtain an estimate for the strength of $Ly\alpha$ emission. A careful analysis of the $H\alpha$ emission from the ring was presented by Pun et al. [12], where they find the $H\alpha$ flux from “Spot 1” (the first observed hotspot) in September 1999 to be $1.8 \times 10^{-14} \text{ ergs cm}^{-2} \text{ s}^{-1}$, which translates into a photon flux at $Ly\alpha$ of $0.03 - 0.06 \text{ photons cm}^{-2} \text{ s}^{-1}$. This flux will be several times greater at the time of the most recent $Ly\alpha$ observations presented here (see Figure 5). A rough measurement of the $H\alpha$ hotspot emission within the *STIS* slit in the 2010 observations ($\approx 2.1 \times 10^{-12} \text{ ergs cm}^{-2} \text{ s}^{-1}$) suggests that the hotspot $Ly\alpha$ flux in 2010 is approximately 3–7 $\text{photons cm}^{-2} \text{ s}^{-1}$. This number is sufficient to account for the broad blueshifted $Ly\alpha$ emission seen in Figure 4.

Regarding the question of optical depth in the line wings of $Ly\alpha$, the radial column density of hydrogen atoms in the debris is roughly $N_H \approx M_H / (4\pi R^2 m_H)$, where we estimate that the mass of hydrogen in the supernova envelope, $M_H \sim 5M_\odot$, $R \approx 6 \times 10^{17} \text{ cm}$ is the radius of the envelope, and m_H is the mass of the hydrogen atom. With these estimated values, we find $N_H \approx 1.3 \times 10^{21} \text{ cm}^{-2}$. The optical depth of such a column to $Ly\alpha$ photons, Doppler shifted by $v_{1000} = v/(1000 \text{ km s}^{-1})$, is given roughly by $\tau \approx N_H \sigma_o ((\gamma/4\pi^2) / (\Delta f^2 + (\gamma/4\pi)^2))$ [23], where the frequency shift is $\Delta f/f_0 = v/c$, σ_o is the line center absorption cross section, and $\gamma = 6.3 \times 10^8 \text{ s}^{-1}$ is the spontaneous decay rate of electrons in the excited state of the hydrogen atom leading to the emission of $Ly\alpha$ photons. Evaluating this expression at $v_{1000} = -6$, we find that $\tau \approx 0.1$. For comparison, we estimate $\tau > 2.5$ for $|v_{1000}| < 1$. (Note that a $Ly\alpha$ photon moving sideways along a chord through the supernova debris will encounter a greater optical depth.) It should be noted that we do not include a reduction in the effective $Ly\alpha$ optical depth due to dust attenuation in the supernova debris. Uncertainties in the amount of dust in the inner remnant, as well as in the far-UV optical properties of such grains conspire to make such an attenuation factor highly speculative. The gas-to-dust ratio is most likely substantially smaller than the typical diffuse interstellar medium, thus a conservative estimate of the $Ly\alpha$ attenuation would be factors of a few. Our estimate of the available $Ly\alpha$ photon budget from the hotspots provides ample margin for this mechanism to operate. Thus, even given the uncertainty regarding the degree to which dust contributes to the local optical depth, we conclude that a measurable fraction of the $Ly\alpha$ photons that are emitted by a hotspot and enter the supernova debris will be backscattered and emerge with blueshifts ranging up to $\sim -12,000 \text{ km s}^{-1}$.

5. N v $\lambda\lambda 1239, 1243 \text{ \AA}$ Emission?

Figure 5 shows the brightening of the $Ly\alpha$ emission from 2004 to 2010. An interesting feature is the faint glow seen on the north and south sides at wavelengths ranging from $\sim 1260 - 1290 \text{ \AA}$, also visible in Figure 3. This emission cannot be attributed to $Ly\alpha$, because it requires the $Ly\alpha$ emission on the north side to be redshifted by velocities up to $+20,000 \text{ km/s}$, while the actual $Ly\alpha$ emission on that side is blueshifted (Figures 3, 4 and 5).

Instead, we believe that this emission comes from fast-moving N^{4+} ions (observed in the N v $\lambda\lambda 1239, 1243 \text{ \AA}$ resonance doublet) in a thin layer immediately downstream from the reverse shock. Neutral or singly-ionized nitrogen atoms that cross the reverse shock and enter the shocked plasma are repeatedly ionized by collisions in the shock transition zone. As it passes through the Li-like ionization stage (N^{4+}), a nitrogen atom may be excited to the 2^1P fine structure state and emit a N v 1239 \AA or 1243 \AA photon, or it

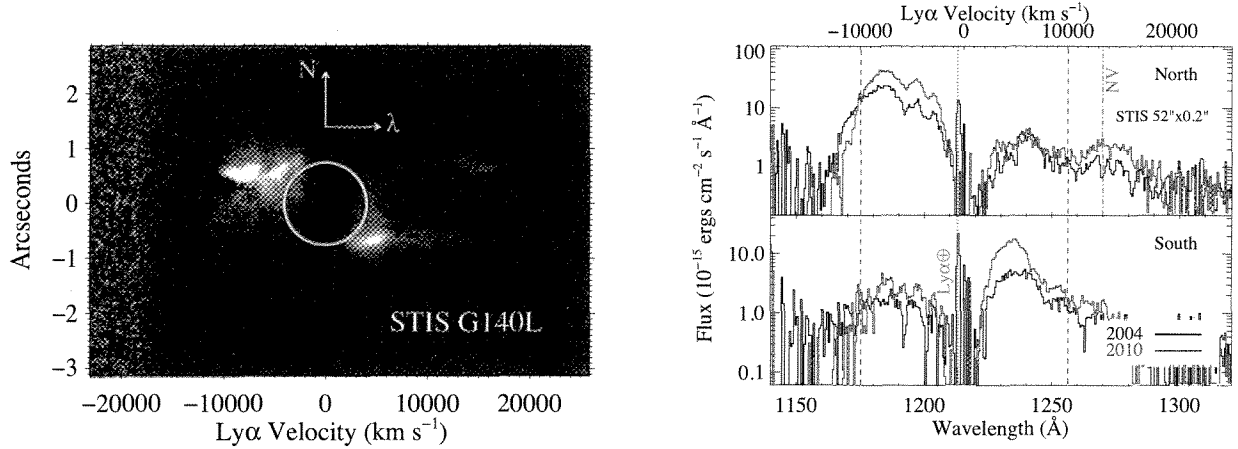


Figure 5: At *left*, we display the Ly α 2010-2004 difference image, scaled such that black indicates similar intensities in the two epochs. The yellow circle approximates the location of the circumstellar emission ring. We quantify the evolution in the spectra (*right*) by displaying one-dimensional spectra of the Ly α emission from the North and South regions. Note that if one attributes the faint red-shifted features to N v $\lambda\lambda 1239, 1243$ Å, one should subtract 6150 km s $^{-1}$ from the Ly α velocity scale to measure the corresponding Doppler shift. We observe two primary features: (a) the Ly α emission has increased in brightness by factors of 1.6–2.4 for the North and South shock emission, indicative of an increased flux of hydrogen atoms into the shock region, and (b) The maximum Doppler shift in the northern blue shifted Ly α emission is decreasing as a function of time. The narrow feature labeled “ \oplus ” is residual emission from Earth’s upper atmosphere, and dashed vertical lines at ± 10000 km s $^{-1}$ have been added for reference.

may be ionized to N $^{5+}$. The number of N v photons produced, per nitrogen atom passing through the reverse shock, will be equal to the ratio of the N $^{4+}$ 2 1 P excitation rate to its ionization rate. But, unlike hydrogen atoms, for which the Ly α excitation rate is about equal to the ionization rate, the excitation rate producing the N v emission (which is dominated by collisions with protons and alpha particles) exceeds the ionization rate by a factor of several hundred [24, 25]. Extrapolating these results to greater shock velocities, we estimate that each nitrogen atom that passes through the reverse shock will emit ~ 600 N v photons before it becomes fully ionized. Given the enriched abundance of nitrogen (atomic ratio N/H $\sim (2 \times 10^{-4})$ [5, 26, 27, 28] in the equatorial ring (and presumably in the outer debris of SN 1987A), it follows that the ratio of observed fluxes of N v to H α (including a factor of 5.3 to account for interstellar extinction of N v) should be of order unity [25]. In fact, if we attribute the redshifted emission observed on the north side of the reverse shock in Figure 3 to N v, and compare this value to the flux of H α seen in the blueshifted streak in Figure 1, we find an observed flux ratio N v/H $\alpha \sim 4$. This ratio is actually an underestimate of the actual flux ratio, since only about half of the N v emission appears in the redshifted blur. The other half of the N v emission will appear in a blueshifted feature that cannot be distinguished because of the larger flux from the blueshifted Ly α emission.

How do we account for the fact that the observed ratio of the redshifted emission feature in the north side of Figure 3 to H α is greater than the expected ratio of N v to H α ? One possible explanation is that most of the hydrogen atoms in the supernova debris are photoionized by radiation from the shocked ring before they reach the reverse shock and thus do not produce H α radiation when they cross the shock. Smith et al. [19] have predicted that this mechanism will become dominant between 2012 and 2014. They estimated the intensity of ionizing radiation by fitting a model of the ionizing radiation to the observed X-ray flux from the shocked gas. But it is possible that the ionizing radiation could be substantially greater than their estimate if it is dominated by shocks entering the circumstellar ring that are too slow to produce the observed soft X-rays.

But why should the N v emission seen on the north side of the reverse shock be redshifted, while H α and Ly α are blueshifted? In contrast to the hydrogen atoms, which are not deflected significantly from free expansion when they emit Ly α , the nitrogen atoms are ionized and deflected by the turbulent electromagnetic fields in the isotropization zone of the collisionless shock before they emit N v photons. However, the N $^{4+}$ ions are not thermalized by collisions with ions and electrons in the shocked plasma. One can easily estimate that the timescale for N $^{4+}$ ions to be slowed by Coulomb collisions in the plasma is some two orders of magnitude greater than the timescale for them to be ionized to N $^{5+}$ [24, 25].

The actual velocity distribution function of the N v ions in this zone is unknown. Figure 6 illustrates a highly idealized model, in which the N $^{4+}$ ions do not lose energy but they gyrate about a magnetic field that is parallel to the shock and moving with the fluid velocity of the shocked plasma. Thus, for example, if nitrogen atoms cross a stationary reverse shock with normal velocity $v_s = 9000$ km s $^{-1}$ and they enter a plasma moving at $v_s/4 = 2250$ km s $^{-1}$, the resulting N $^{4+}$ ions will gyrate with circular velocity 6750 km s $^{-1}$. If the normal to the shock surface is inclined at 45°, as on the N side of the equatorial ring, the Doppler velocity of the N v emission will range from -8341 km s $^{-1}$ to $+5159$ km s $^{-1}$. The distribution function of the projected velocities will peak at these extremes.

If our identification of this faint feature as N v is correct, we are actually seeing redshifts on the north side extending to $\sim 12,000$

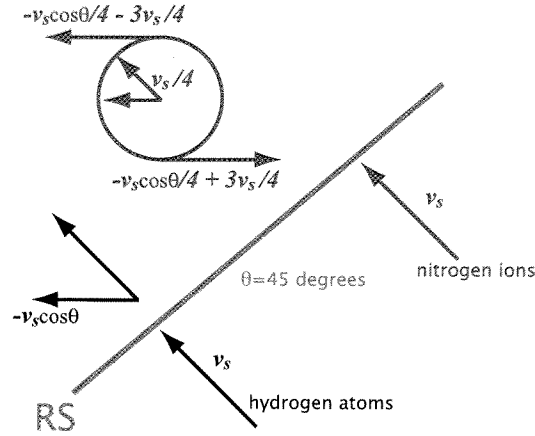


Figure 6: Schematic illustrating how the line profile of N v $\lambda\lambda 1239, 1243 \text{ \AA}$ may differ from that of Ly α . The hydrogen atoms (velocity vectors in black) cross the reverse shock surface with velocity v_s and are excited by collisions without significant deflection. Therefore, the Doppler shift seen by an observer to the left is $-v_s \cos \theta$ ($\theta \approx 45^\circ$ for the SN 1987A system). Nitrogen atoms also cross the shock with velocity v_s , but they become ionized and gyrate about magnetic fields frozen into the shocked plasma rest frame and moving with velocity $v_s/4$. The purple arrows show the extremes of the Doppler shifts of the N v emission.

km s^{-1} , greater than the simple model of Figure 6 suggests. However, the actual shape and location of the reverse shock are certainly more complicated than those illustrated in Figure 6. Another very interesting possibility is that we may be seeing evidence for particle acceleration in the isotropization zone of the reverse shock. Given the uncertainties mentioned above, we must regard our identification of this faint redshifted feature as N v as speculative. Fortunately, as we describe below, future observations with the *HST* will enable a definitive test.

6. Future Prospects: Deep Observations of SN 1987A with *HST*-COS

There is much to be learned about the reverse shock in SN 1987A from further spectroscopic observations. The shape of the reverse shock surface can be determined in three dimensions from analyzing spectra of H α emission with *STIS* using narrow slits. But the current *STIS* observations view only a strip of the reverse shock surface that cuts through the center of the remnant. To develop a full map of the reverse shock, we will need similar *STIS* observations at about seven parallel slit locations.

Some of the broad Ly α emission from SN 1987A does not have the same source as the broad H α emission. We suggest instead that this emission may result from Ly α emission by the shocked equatorial ring that is reflected by nearly coherent resonant scattering in the freely expanding supernova debris. We have also detected a broad, redshifted emission feature that we attribute to the N v $\lambda\lambda 1239, 1243 \text{ \AA}$ lines, which Borkowski et al. [25] had predicted might be detectable with *STIS*. If this identification is correct, the N v line profile opens a unique, investigative window into the kinetics of a collisionless shock. Unfortunately, the expected blueshifted part of the line profile is overwhelmed by the Ly α emission in our *STIS* observations.

Observations of the ultraviolet spectrum of SN 1987A with the *Cosmic Origins Spectrograph* (COS) can yield new insights into the physics of the reverse shock. COS was installed on *HST* during STS-125/Servicing Mission 4; it is a slitless, modified Rowland Circle spectrograph designed for high-sensitivity, medium-resolution observations in the vacuum-ultraviolet bandpass (1150 – 3200 \AA). Due to its high throughput, COS is a powerful tool for the study of diffuse emission in the Magellanic Clouds [29]. With COS, we will be able to measure the line profiles of Ly α and N v with much better signal-to-noise ratio than possible with *STIS*. It should also enable us to measure profiles of other ultraviolet emission lines from the reverse shock that are too faint to see with *STIS*. For example, the C iv $\lambda\lambda 1548, 1551 \text{ \AA}$ resonance doublet should be detectable with COS. The abundance ratio of carbon to nitrogen is $\text{C/N} \approx 0.2$ in SN 1987A [5], but that is partially offset by a smaller amount of dust attenuation at C iv relative to N v, and we estimate that C iv $\lambda\lambda 1548, 1551 \text{ \AA}$ emission by the reverse shock should be fainter than N v by a factor ~ 3 . C iv should have the same intrinsic line profile as N v, but its redshifted wing will not be confused with Ly α emission and absorption. Observation of the complete line profile of C iv could test whether our identification of N v and its emission mechanism is correct. It may also be possible to detect the velocity-resolved reverse shock profiles of Si iv $\lambda\lambda 1394, 1403 \text{ \AA}$, N iv] $\lambda\lambda 1483, 1487 \text{ \AA}$ and He ii $\lambda 1640 \text{ \AA}$. The full profiles of these transitions are most likely below the background equivalent flux for *STIS*. However, for ultraviolet observations of the very faintest astrophysical emissions ($F_\lambda \lesssim 10^{-16} \text{ ergs cm}^{-2} \text{ s}^{-1} \text{ \AA}^{-1}$), COS is approximately 50 times more sensitive than *STIS*.

Twenty-three years later, SN 1987A still has valuable lessons to offer.

K.F. thanks Matthew Beasley for helpful discussion. Support for this research was provided by NASA through grant GO-11181 from the Space Telescope Science Institute, which is operated by the Association of Universities for Research in Astronomy, Incorporated, under NASA contract NAS5-26555.

References

- [1] Arnett, D., Bahcall, J. N., Kirshner, R. P., & Woosley, S. E. 1989, ARA&A, 27, 629
- [2] McCray, R. 1993, ARA&A, 31, 175
- [3] McCray, R. 2007, AIPC, 937, 3
- [4] Panagia, N., Gilmozzi, R., Macchetto, F., Adorf, H.-M., & Kirshner, R.P. 1991, ApJ, 380, L23
- [5] Lundqvist, P. & Fransson, C. 1996, ApJ, 464, 924
- [6] Grönningsson, P., Fransson, C., Lundqvist, P., Lundqvist, N., Leibundgut, B., Spyromilio, J., Chevalier, R. A., Gilmozzi, R., Kjaer, K., Mattila, S., & Sollerman, J. 2008, A&A, 479, 761
- [7] Crots, A. P., & Heathcote, S. R. 1991, Nature, 350, 683.
- [8] Morris, T., & Podsiadlowski, P. 2007, Science, 315, 1103
- [9] Chevalier, R. A. 1982, ApJ, 258, 790
- [10] Garnavich, P., Kirshner, R. P., & Challis, P., IAU Circular 6710 (30 July 1997)
- [11] Lawrence, S.S., Sugerman, B.E., Bouchet, P., Crots, A.P.S., Uglesich, R. R., & Heathcote, S.R. 2000, ApJ, 537, L123
- [12] Pun, C. S. J., Michael, E., Zhekov, S.A., McCray, R., Garnavich, P.M., Challis, P. M., Kirshner, R.P., Baron, E., Branch, D., Chevalier, R.A., Filippenko, A.V., Fransson, C., Leibundgut, B., Lundqvist, P., Panagia, N., Phillips, M.M., Schmidt, B., Sonneborn, G., Suntzeff, N.B., Wang, L., & Wheeler, J.C. 2002, ApJ, 572, 906
- [13] Heng, K., McCray, R., Zhekov, S.A., Challis, P.M., Chevalier, R.A., Crots, A.P.S., Fransson, C., Garnavich, P., Kirshner, R.P., Lawrence, S.S., Lundqvist, P., Panagia, N., Pun, C.S.J., Smith, N., Sollerman, J., & Wang, L. 2006, ApJ, 644, 959
- [14] Chevalier, R. A., Kirshner, R. P. & Raymond, J.C. 1980, ApJ, 235, 186
- [15] Michael, E., McCray, R., Chevalier, R., Filippenko, A.V., Lundqvist, P., Challis, P., Sugerman, B., Lawrence, S., Pun, C.S.J., Garnavich, P., Kirshner, R., Crots, A., Fransson, C., Li, W., Panagia, N., Phillips, M., Schmidt, B., Sonneborn, G., Suntzeff, N., Wang, L., & Wheeler, J.C. 2003, ApJ, 593, 809
- [16] Heng, K. & McCray, R. 2007, ApJ, 654, 923
- [17] Chevalier, R.A., & Raymond, J.C. 1978, ApJ, 225, L27
- [18] Heng, K. 2010, PASA, 27, 23
- [19] Smith, N., Zhekov, S.A., Heng, K., McCray, R., Morse, J.A., & Gladders, M. 2005, ApJL, 635, 41
- [20] Suntzeff, N. B. & Bouchet, P. 1990, AJ, 99, 650
- [21] Scuderi, S., Panagia, N., Gilmozzi, R., Challis, P.M. & Kirshner, R.P. 1996, ApJ, 465, 956
- [22] Osterbrock, D.E. 1989, Univ. Science Books, 422
- [23] Rybicki, G.B. & Lightman, A.P. 1979, New York, Wiley-Interscience
- [24] Laming, J. M., Raymond, J. C., McLaughlin, B. M., & Blair, W. P. 1996, ApJ, 472, 267-274
- [25] Borkowski, K.J., Blondin, J.M., & McCray, R. 1997, ApJL, 476, 31
- [26] Haberl, F., Geppert, U., Aschenbach, B. & Hasinger, G. 2006, A&A, 460, 811
- [27] Zhekov, S.A., McCray, R., Borkowski, K.J., Burrows, D.N., & Park, S. 2006, ApJ, 645, 293
- [28] Heng, K., Haberl, F., Aschenbach, B. & Hasinger, G. 2008, ApJ, 676, 361
- [29] France, K., Beasley, M., Keeney, B.A., Danforth, C.W., Froning, C.S., Green, J.C., & Shull, J.M. 2009, ApJL, 707, 27